

REGULAR PAPER

## Validation of damage on vascular endothelial cells under ultrasound exposure according to adhered situation of bubbles

To cite this article: Yoshiki Ito *et al* 2022 *Jpn. J. Appl. Phys.* **61** SG1066

View the [article online](#) for updates and enhancements.

### You may also like

- [Observation of cavitation bubbles and acoustic streaming in high intensity ultrasound fields](#)  
Yuuki Uemura, Kazuma Sasaki, Kyohei Minami *et al.*
- [Ultrasound exposure conditions for suppressing survival of human glioblastoma U-87MG cells](#)  
Akiko Watanabe, Sakino Iwashiro, Masatsune Minai *et al.*
- [Highly efficient cavitation-enhanced heating with dual-frequency ultrasound exposure in high-intensity focused ultrasound treatment](#)  
Hiroshi Sasaki, Jun Yasuda, Ryo Takagi *et al.*



## Validation of damage on vascular endothelial cells under ultrasound exposure according to adhered situation of bubbles

Yoshiki Ito<sup>1</sup>, Tatsuya Saito<sup>1</sup>, Shunya Watanabe<sup>1</sup>, Naoya Kajita<sup>1</sup>, Yoshitaka Miyamoto<sup>2</sup>, Ryo Suzuki<sup>3,4</sup>, Kazuo Maruyama<sup>3,4</sup>, Daiki Omata<sup>3</sup>, and Kohji Masuda<sup>1\*</sup>

<sup>1</sup>Graduate School of BASE, Tokyo University of Agriculture and Technology, Koganei, Tokyo 184-8588, Japan

<sup>2</sup>National Center for Child Health and Development, Setagaya, Tokyo 157-8535, Japan

<sup>3</sup>Faculty of Pharma-Science, Teikyo University, Itabashi, Tokyo 173-8605, Japan

<sup>4</sup>Advanced Comprehensive Research Organization (ACRO), Itabashi, Tokyo 173-8605, Japan

\*E-mail: [ultrason@cc.tuat.ac.jp](mailto:ultrason@cc.tuat.ac.jp)

Received November 3, 2021; revised January 18, 2022; accepted January 20, 2022; published online May 31, 2022

We investigated the viability of vascular endothelial cells with the existence of lipid bubbles under ultrasound exposure. First, we estimated the various situations of bubbles on the cells including either adhesion, floating, or both of them using not only image analysis but also an experiment to retain the cells in flow. Then we examined the viability measurement of the cells using the ultrasound conditions with the frequency of 3 MHz, a maximum sound pressure of 400 kPa pp, and a maximum irradiation time of 60 s. We found that the floating bubbles caused more damage on the cells rather than the adhered bubbles. Because insufficient adhesion of bubbles might cause damage by floating bubbles, we consider that the adhered bubbles were protective of cells against floating bubbles. However, excessive bubbles with a higher concentration than the saturation also might cause damage by destructing both the floating and adhered bubbles. © 2022 The Japan Society of Applied Physics

### 1. Introduction

Microbubbles and nanobubbles have been utilized for physical drug delivery to allow the uptake of large molecules into cells, where the ease in determining the distribution of bubbles functioning as a contrast agent in blood flow is advantageous. To prevent the diffusion of bubbles after injection into the human body and reduce side effects such as relapse and metastasis inhibitory effects, we have been researching a method to control bubbles<sup>1-4</sup> using acoustic radiation force. Additionally, we have been researching the manipulation of therapeutic cells to contribute to cellular immunotherapy,<sup>5-7</sup> wherein bubble-surrounded cells (BSCs)<sup>8-14</sup> are produced by attracting bubbles on the cell surfaces to reduce their density. These previous studies have shown that micro objects in blood vessels can be controlled by performing active induction in a bifurcated path using a standing wave<sup>13,14</sup> and active retention in the middle of a path using a travelling wave.<sup>15-19</sup> In an actual situation, a catheter should be used to place the micro objects close to the target area. Once micro objects are released from the tip of the catheter,<sup>20,21,22</sup> they are exposed to a sound pressure of several 100 kPa. When tempo-spatial division emission,<sup>17,19,21,22</sup> which generates multiple focal points by temporally and spatially distributing acoustic energy, is applied, emission duration and duty ratio should be primarily considered for an effective performance.

In the above situations, since blood vessel walls are exposed to ultrasound during the control of micro objects, the biological effect on vascular endothelial cells should be considered. Moreover, the cells might be damaged due to cavitation caused by bubbles collapse. To understand the biological effect on the cells, some studies have analyzed the damage caused to cells by low-intensity pulsed ultrasound (LIPUS),<sup>23,24</sup> wherein the expression factors to induce cell formation, which promote cell proliferation, were examined under ultrasound exposure. One previous study estimated the growth of staphylococcus epidermidis with respect to ultrasound irradiation.<sup>25</sup> Additionally, studies have been conducted to estimate the effects of ultrasound irradiation on

endothelial and cancer cells in the absence of bubbles<sup>26</sup> However, the damage to vascular wall under ultrasound exposure in the presence of bubbles has not been clearly elucidated. Furthermore, using an appropriate ligand, since bubbles can adhere to cell surfaces, a new therapeutic application can be managed by verifying whether the adhered bubbles enhance or reduce the damage to cells. In this study, we investigate the biological damage on vascular endothelial cells and the concentration and adhesion of bubbles under various conditions of ultrasound exposure.

### 2. Experimental methods

#### 2.1. Cells and bubbles

In this research, we employed bovine-derived carotid epithelial HH cells (cells, hereinafter) obtained from the Japan Cell Research Bank. They were cultured at 37 °C and a CO<sub>2</sub> concentration of 5%, using Eagle's minimal essential medium with 10% fetal calf serum<sup>27</sup> When the culture reached confluence, it exhibited a typical cobblestone structure. Additionally, we used lipid bubbles (LBs), containing perfluoropropane (PFP, C<sub>3</sub>F<sub>8</sub>) gas and composed of 1,2-distearoyl-sn-glycero-3-phosphatidyl-choline (DSPC) and 1,2-distearoyl-sn-glycero-3-phosphatidyl-ethanolamine-polyethylene glycol 2000 (DSPE-PEG2k).<sup>4,28,29</sup> DSPC:DSPE-PEG2k in the molar ratio of 94:6 was dissolved in mixed organic solvents (each containing 4 ml of chloroform) and then 4 ml phosphate buffered saline (PBS) was added into the lipid solution and sonicated using a bath type sonicator for 3 min. After the removal of the organic solvent via evaporation, the LB suspension was filtered through a 0.45 μm filter. The obtained LBs had an average diameter of 100 nm and were encapsulated with the phosphate buffer solution in a liposome.

Thereafter, we prepared modified LBs by conjugating cyclic-RGD (cyclo Arg-Gly-Asp-D-Phe-Cys, cRGD) peptides,<sup>30-32</sup> which covalently adhere to vascular endothelial cells via DSPE-PEG3.4k on the LB surfaces. The conjugation between DSPE-PEG3.4k-Mal and cRGD was executed under incubation for 1 h at room temperature and overnight at 4 °C using a rotary mixer.

In the following description, the modified LBs are denoted as “LBs (+)” and the original ones are denoted as “LBs (–).” In LBs (+), the molar ratio of DSPC:DSPE-PEG2k:DSPE-PEG3.4k-cRGD was 94:5:1; thus, both LBs were mainly composed of DSPC. Since the molecular weight of the conjugation, which was extended to the outside of the DSPC sphere, was heavier than that of DSPE-PEG2k, the physical strength of LBs (+) is expected to be similar or more fragile than that of LBs (–). Similar to our previous study,<sup>12–14</sup> we formed bubble-surrounded cells (BSCs) using the LBs (+).

To prepare the LB suspension, 2 ml of liposome suspension (lipid concentration: 1 mg ml<sup>-1</sup>) was diluted to yield the desired PBS concentration, where the concentration [mg ml<sup>-1</sup>] was derived from the weight of lipid divided by the volume of suspension. For the optical observation of BSCs, the cells were dyed with tetramethyl rhodamine, which emits a distinct fluorescence with a wavelength of 570 nm under a 548 nm excitation light, to distinguish them during fluorescence observation. Then, the bubbles were dyed with DiO, which emits a distinct fluorescence with a wavelength of 501 nm under a 484 nm excitation light.

**2.2. Retention of bubble-surrounded cells in flow**

Since the controllability of BSCs is better for cells with LBs (+) attached onto the cell surfaces than that for cells without LBs according to ultrasound exposure,<sup>10–12</sup> we attempted to estimate the degree of adhesion of LBs onto cells by retaining BSCs in flow under ultrasound exposure. Our preceding studies<sup>8–12</sup> suggested that a propelling force to the cell is enhanced by the travelling wave reflected on the surface of the cell because of the boundary in the acoustic impedance. Furthermore, oscillation of the bubbles also enhances the Bjerknes force to propel the cell in the direction of the travelling wave. In the previous study<sup>12</sup> the retained cells were optically observed in the middle of the flow under focal exposure of ultrasound, where the amount of the cells retained reflects the adhered LBs onto cells. Figure 1 shows the vertical view of the experimental setup, including an industrial microscope (Olympus, BXFM), a digital camera (Olympus, DP74), an ultrasound transducer, a water tank, and an artificial blood vessel. At the bottom of the water tank, which was filled with degassed water, an ultrasound transducer with a concave ceramic disc with a central frequency of 3 MHz was set with a dip angle  $\theta = 60^\circ$  to afford a focal wave to retain the cells in the middle of the flow. The distance between the path and transducer was  $l = 65$  mm,

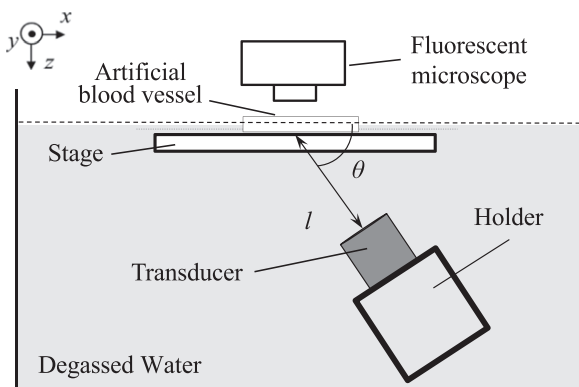


**Fig. 1.** Experimental setup for observing behavior of the BSCs including a transducer and a fluorescence microscope.

which corresponds to the near-field limit of the transducers. The maximum sound pressure was limited to 400 kPa pp. Here, the sound pressure distribution was measured using an acoustic intensity measurement system (Onda AIMS III) by translating the hydrophone (Onda HNR- 1000) in degassed water. The beam width (half-width of the sound pressure distribution) was 2.5 mm. The artificial blood vessel, which was composed of polyvinyl alcohol (PVA) and had a sound velocity of 1550 m s<sup>-1</sup> and density of 1.2 g ml<sup>-1</sup>, was placed on the stage for position adjustment. The path width in the artificial blood vessel was 1 mm.

**2.3. Ultrasound irradiation to the cells and lipid bubbles suspension**

Figure 2 shows the experimental setup for exposing the cells and LBs suspension to ultrasound echography. A 96-well plate was placed on the water surface; the water temperature was maintained at 37 °C. The suspension was poured into multiple wells, one of which had a diameter of 6 mm and a depth of 10 mm (0.3 ml well<sup>-1</sup>). The maximum amount of suspension was fixed to 0.1 ml to leave room for additional reagents after ultrasound exposure. At the bottom of the water tank, which was filled with degassed water, two or three identical ultrasound transducers with a flat ceramic disc with a central frequency of 3 MHz were placed to emit a plane continuous or burst wave to a well at a distance  $l = 65$  mm. An  $x$ – $y$  stage was installed to move the plate in the horizontal direction. To avoid unwanted ultrasound exposure to a neighboring well, alternate wells on the plate were used.

In order to measure cell viability after ultrasound exposure, we have introduced conventional cell assays of Cell Counting Kit-8 (CCK-8)<sup>13,33</sup> by counting the number of viable cells in the culture wells. The cells in the plates were incubated for 24 h after ultrasound exposure, and then CCK-8 was injected into each well as a reagent for measuring absorbance, to determine cell viability.

**3. Results**

**3.1. Fluorescent observation of floating bubbles**

Before performing the BSCs retention in flow experiment under ultrasound exposure, we optically observed the brightness of LBs using an industrial microscope (Olympus, BX53) and a digital camera (Photometrics, Cool SNAP EZ). The cell

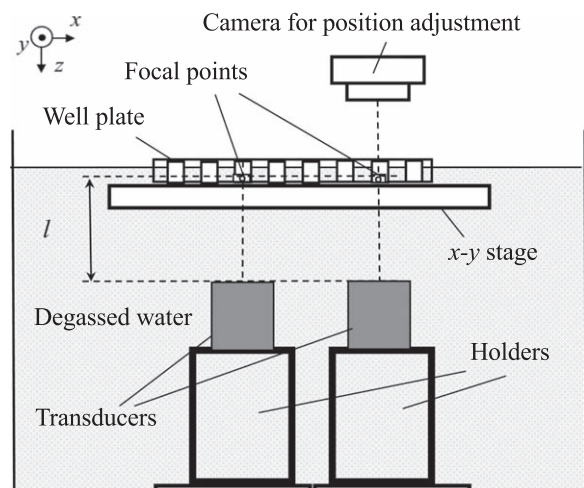


**Fig. 2.** Experimental setup to expose ultrasound to suspension in wells including multiple transducers.

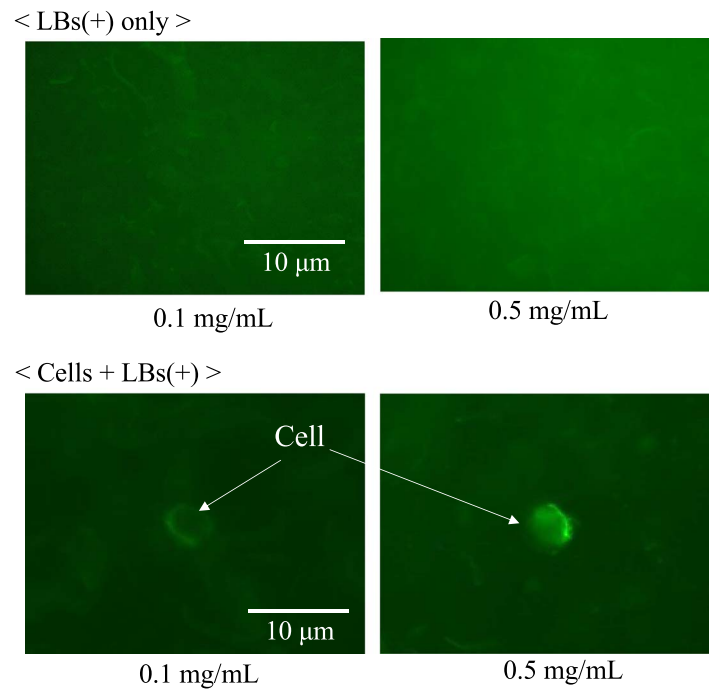


**Fig. 3.** (Color online) Fluorescent images of lipid bubbles (LBs) captured by a confocal microscope and optically filtered to only bubbles; LBs only (upper) and cells and LBs (lower) with the concentration of LBs of 0.1 mg ml<sup>-1</sup> (left) and 0.5 mg ml<sup>-1</sup> (right).

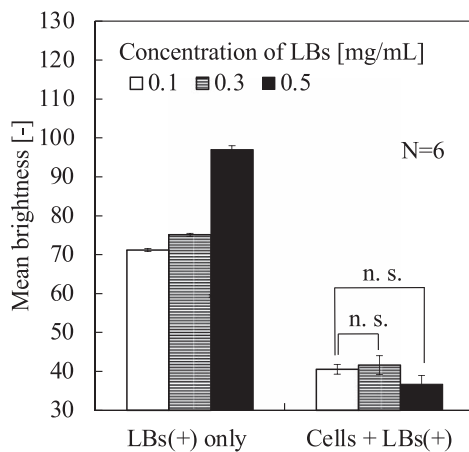


**Fig. 4.** Comparison of background brightness on the microscopic images of LBs shown in Fig. 3, where the error bars indicate the standard deviation.

concentration was fixed as  $1.0 \times 10^5 \text{ ml}^{-1}$ . Figure 3 shows the obtained images that were optically filtered to obtain only bubbles (green); the upper two photos present only LBs (+) and the lower two photos present BSCs with LB concentrations of 0.1 and 0.5 mg ml<sup>-1</sup>. In the lower photos, as the LBs were taken to the cell surface, the distribution of floating LBs was much thinner than that in the upper photos. Figure 4 shows the mean brightness of floating LBs versus the concentration of LBs for each condition, where six photos were used for each calculation. Without the cells, the brightness increased according to the LBs concentration. However, in BSCs, no significant difference in the mean brightness (except the area of cells) was observed with use of a t-test between the concentrations of 0.1 and 0.5 mg ml<sup>-1</sup>, suggesting that the amount of adhered LBs on the cell surfaces was not saturated in the experimented concentration

of LBs. In other words, there is still room for LBs on the cell surfaces in those concentrations.

**3.2. Retention of bubble-surrounded cells in flow**

To support the assumption stated in the previous section, we performed the retention experiment using the experimental setup shown in Fig. 2. The transducer irradiates a burst wave with a maximum sound pressure of 400 kPa pp, a duty ratio of 60%, and a pulse repetition frequency of 0.1 ms. The BSC suspension comprised a fixed concentration of the cells ( $1.0 \times 10^5 \text{ ml}^{-1}$ ), where the concentration of LBs (+) was varied from 0.1 to 0.5 mg ml<sup>-1</sup>. Figure 5 shows the fluorescent images of the retained cells in BSCs 30 s after the ultrasound exposure was started at a flow velocity of 10 mm s<sup>-1</sup>. The retained area of the cells increased in proportion to the LB concentration.

Figure 6 shows the variation of the retention area of the cells versus the concentration of LBs, where the retention area was calculated by thresholding the brightness to 78 determined by the brightness of background. The error bars in Fig. 6 indicate the standard deviation of the retention area obtained in 4 attempts. Clearly, the existence of the adhered LBs on the cell surfaces enhanced the performance and propelled the cells to the vessel wall. Furthermore, as confirmed in Fig. 3, since the concentrations of floating bubbles, which did not adhere and exist near the cells, were similar between 0.1 and 0.5 mg ml<sup>-1</sup>, the effect of the floating LBs can be ignored in the results of Fig. 6. The saturation of the retention area with LB concentrations of >0.5 mg ml<sup>-1</sup> suggests that the adhesion of LBs on the cells saturated at the concentration of 0.5 mg ml<sup>-1</sup>. Considering the results through Figs. 3 and 6, where the concentration of the cells was fixed to  $1.0 \times 10^5 \text{ ml}^{-1}$ , when the LBs concentration was 0.1 mg ml<sup>-1</sup>, the LBs (+) in the suspension certainly adhered onto the cell surfaces, but the adhesion was insufficient to afford the necessary retention

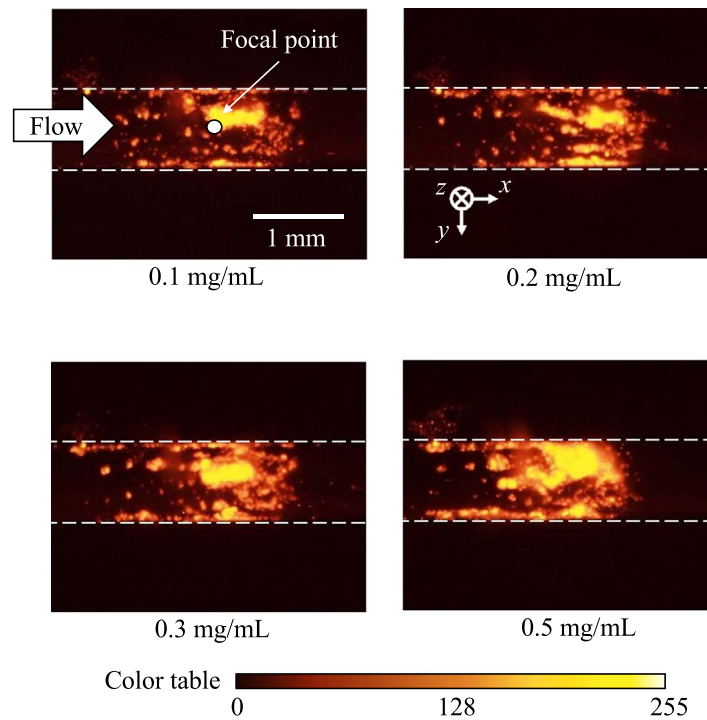


**Fig. 5.** (Color online) Fluorescent images of retained cells included in BSCs in 30 s after the starting of injection of the suspension of cells and LBs (+) at a flow velocity of  $10 \text{ mm s}^{-1}$  under continuous ultrasound emission with 400 kPa pp at a frequency of 3 MHz, where the concentrations of LBs were designated.

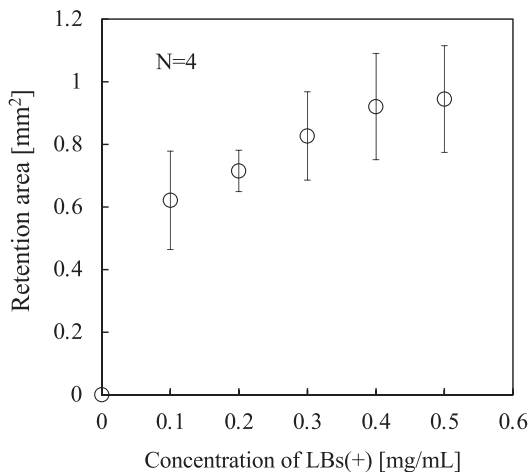
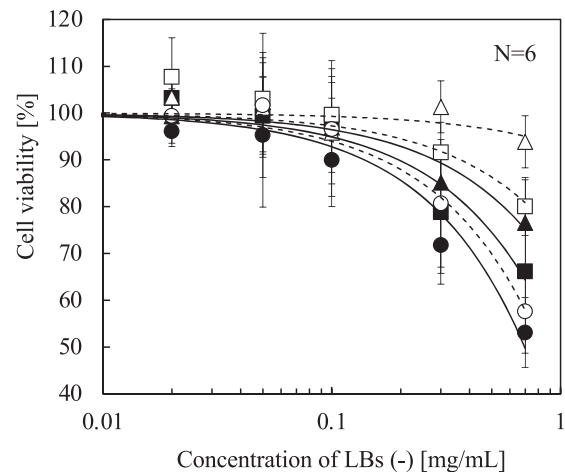


**Fig. 6.** Retained area of the cells versus concentrations of LBs (+) derived from Fig. 5, where the error bars indicate the standard deviation.

performance and the cells possessed the ability to take more LBs.

### 3.3. Cell viability under ultrasound exposure in the presence of lipid bubbles

Next, we analyzed the damage on the cells caused by the floating LBs near the cells under ultrasound exposure and compared with the various conditions of LBs adhesion on the cells. Here, we prepared various concentrations of the LBs (-) with a fixed cell concentration of  $1.0 \times 10^5 \text{ ml}^{-1}$ . Figure 7 shows the cell viability versus the LBs (-) concentration when the cells were irradiated with a central frequency of 3 MHz, a sound pressure of 300 or 400 kPa pp, and a duty ratio of either 30%, 60%, or 100%. Pulse repetition time was fixed to 0.1 ms. Solid and dashed lines were approximated with a linear function using the least squares method. The error bars in Fig. 7 indicate the standard deviation of the cell viability obtained in 6 attempts. In the



Sound pressure [kPa-pp]	Duty ratio [%]		
	30	60	100
300	---△---	---□---	---○---
400	---▲---	---■---	---●---

**Fig. 7.** Cell viability under exposure of a burst wave versus concentrations of LBs (-) according to a sound pressure and a duty ratio at a frequency of 3 MHz.

presence of the floating LBs, the cell viability decreased with the sound pressure and the duty ratio, whereas the cell viability was almost 100% without LBs. The damage on the cells was confirmed by the presence of LBs as well as T-cells<sup>13)</sup>

Finally, we performed the above experiment using the LBs (+) with various adhesion conditions on the cells. Figures 8 shows the cell viability versus the total LBs concentration. The cells were irradiated using the ultrasound conditions, which most affected the damage to the cells in Fig. 7, with a

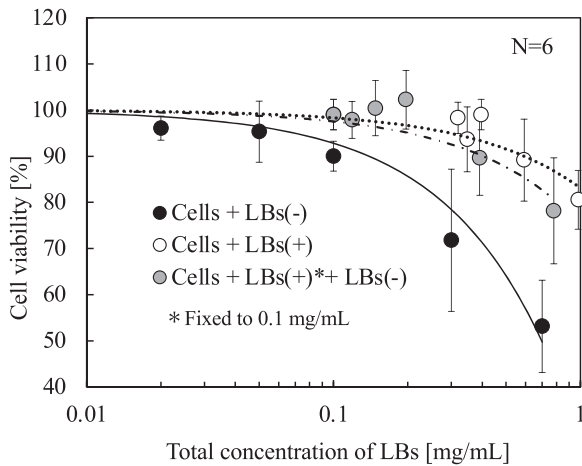


**Fig. 8.** Cell viability under exposure of a continuous wave versus total concentration of LBs in presence of LBs (–), LBs (+), and both of them according to a sound pressure and a duty ratio at a frequency of 3 MHz.

central frequency of 3 MHz, a sound pressure of 400 kPa pp, and a duty ratio of 100%<sup>32</sup> Pulse repetition time was fixed to 0.1 ms. Solid and dashed lines were approximated with a linear function using the least squares method. The error bars in Fig. 8 indicate the standard deviation of the cell viability obtained in 6 attempts. The plot of LBs (+) was similar to that of LBs (–) in Fig. 7. Notably, when the LBs (–) were replaced with the LBs (+), a significant recovery of the cell viability was observed where the LBs (+) concentration was more than 0.3 mg ml<sup>–1</sup>. Moreover, to verify those results, we examined a suspension of the cells and the LBs (+), with fixed concentrations of  $1.0 \times 10^5$  ml<sup>–1</sup> and 0.1 mg ml<sup>–1</sup>, respectively, before injecting various concentrations of the LBs (–) suspension. As shown in Fig. 8, where the horizontal axis indicates the total concentration of the LBs (+) and LBs (–), the cell viability curve is present between the curves of the LBs (–) and the LBs (+), denoting that the adhered LBs (+) acted toward reducing the cell damage.

#### 4. Discussion

In the experiment stated in Sect. 3.1, we estimated the adhesion of LBs on the cells. Because of the significant difference in the mean brightness between “LBs (+) only” and “Cells + LBs (+)” with the concentration of the LBs (+) of 0.1 mg ml<sup>–1</sup> in Fig. 4, it clearly shows that the LBs adhered on the cells when the cells were contained in the suspension. However, no significant difference was observed in the mean brightness of the floating LBs between the concentration of the LBs (+) of 0.1 mg ml<sup>–1</sup> and 0.5 mg ml<sup>–1</sup> when the cells were contained in the suspension. If there is a room for LBs on the surface of the cells with the concentration of the LBs (+) of 0.1 mg ml<sup>–1</sup>, the mean brightness of the floating LBs should decrease with the LB concentration. To explain the above inconsistency, we consider the following two possibilities: (1) the mean brightness in the background was caused by free dye that is independent from the floating LBs or (2) a certain amount of LBs without the conjugated ligand (cRGD) were present.

Additionally, considering the experimental results in Sect. 3.2, the adhesion of the LBs to the cells is clearly insufficient with the LBs (+) concentration of 0.1 mg ml<sup>–1</sup>

because of the decrease in the cell controllability. Therefore, in either of the above assumptions, the adhesion amount of LBs (+) with 0.1 mg ml<sup>–1</sup> should be 20% or less than that with 0.5 mg ml<sup>–1</sup>. Considering the above results, we regarded the LBs (+) concentration of 0.1 mg ml<sup>–1</sup> as insufficient adhesion on the cell surface, where the LBs did not completely cover the cell surfaces.

In the experiment stated in Sect. 3.3, we investigated the influence of the presence of LBs (–) on the cells under ultrasound exposure, as shown in Fig. 7, which is important in that we have confirmed that the LBs react to ultrasound parameters and have the potential to affect the cells. Similar to our previous study<sup>13)</sup> that was conducted using T-cells with a frequency of 3 MHz, we obtained a similar tendency: the cell viability under ultrasound exposure decreased with the LBs concentration, sound pressure, and duty ratio. This suggests that the destruction of the LBs causes damage to the cell surfaces. In proportion to the concentration of the LBs, the distances between the cells and the LBs would be closer. Note that in some conditions the cell viability increased, where the cell viability increases with duty ratios lower than 60% and a sound pressure of 300 kPa pp. Therefore, the possibility of enhancing cell viability using ultrasound and LBs needs to be investigated.

Based on Fig. 8, since significant difference existed in the cell viability between the LBs (+) and the LBs (–) even when they were present in the same concentrations, the adhered LBs were less destroyed under ultrasound exposure than the floating LBs. Additionally, since the LBs (+) are supposed to be more fragile than the LBs (–) due to the attached ligand, as stated in the Sect. 2.1, the oscillation of LBs was suppressed by the adhesion on the cells. The cell viability with the LBs (+) decreased when the LBs concentration was more than 0.5 mg ml<sup>–1</sup> because of the floating LBs, which were not able to adhere on the cells because of saturation and exhibited the same effect as LBs (–). However, because the adhered LBs acted to defend the cells from the destruction of the floating LBs, the damage on the cells was suppressed. This hypothesis can also be explained from the results using the concentrations of the LBs (+) of 0.1 mg ml<sup>–1</sup> and additional LBs (–). As discussed above, when the concentration of the LBs (+) was 0.1 mg ml<sup>–1</sup>, since the LBs did not fully cover the cell surfaces, the cells were damaged by the floating LBs through the surface without the adhered LBs. Therefore, we confirmed that the adhered LBs protected cells from the floating LBs. When the adhesion amount of the LBs was less than the adhesion saturation, the cells were damaged by the floating LBs, if they existed. Alternatively, when the adhesion amount of the LBs was more than the adhesion saturation, the floating LBs caused damage on the cells by destroying the adhered LBs.

In this study, because the cells were floated in a suspension, there is a possibility that the cells can move to reduce the external force caused by the travelling wave, whereas the cells are suppressed in an in vivo situation. However, on the other hand, because the entire surface of the cells was exposed to be affected by floating bubbles around the cells, it can be said that the cells in this study were in a more severe situation than in vivo cells. Although we consider that both effects to increase and decrease cell viability were included, it was possible to investigate the

effect of the cells with respect to the concentration of bubbles and the irradiation conditions of ultrasound. We are going to compare with the results of fixed cells through similar experiments in the future.

From the results obtained in this research, we elucidated a measure to protect vascular endothelial cells from ultrasound irradiation by varying adhesion situations of LBs. In our preceding studies,<sup>8–21,22)</sup> in which we examined active control of micro objects in an artificial blood vessel, we concentrated to irradiate ultrasound to those objects without considering damage on the blood vessels. For the development of therapeutic system including active control of micro objects in blood vessel, the results obtained in this research should be important. Because we have already developed a user interface to recognize three-dimensional structure of the vascular network,<sup>33)</sup> we are going to develop a total diagnosis and treatment system by ultrasound alone.

## 5. Conclusions

In this study, we examined the viability of vascular endothelial cells constituting blood vessels in various conditions of bubbles adhesion under ultrasound exposure. First, we estimated the adhesion situation of bubbles on the cells using not only analysis of fluorescent images but also an experiment to retain the cells in flow. From those experimental results, we determined that floating bubbles cause more damage to the cells than the adhered bubbles. We consider that the adhered bubbles were protective of cells against floating bubbles. However, insufficient adhesion of the bubbles might cause cell damage due to the floating bubbles, and excessive bubbles with a higher concentration than the saturation might also cause cell damage due to the destruction of both floating and adhered bubbles.

## Acknowledgments

This research was supported by a grant from the Japan Society for the Promotion of Science (JSPS) through KAKENHI Grant Number 20H04547.

- 1) V. Garbin, M. Overvelde, B. Dollet, N. De Jong, D. Lohse, and M. Versluis, *Phys. Med. Biol.* **56**, 6161 (2011).
- 2) Y. Yamakoshi and T. Miwa, *Jpn. J. Appl. Phys.* **50**, 07HF01 (2011).
- 3) Y. Yamakoshi, Y. Koitabashi, N. Nakajima, and T. Miwa, *Jpn. J. Appl. Phys.* **45**, 4742 (2006).
- 4) H. Wada, J. Koido, S. Miyazawa, T. Mochizuki, K. Masuda, J. Unga, Y. Oda, R. Suzuki, and K. Maruyama, *Jpn. J. Appl. Phys.* **55**, 07KF06 (2016).
- 5) S. Enosawa, T. Yamazaki, H. Kohsaka, and T. Tokiwa, *Cell Transplant.* **21**, 447 (2012).
- 6) R. A. Fisher and S. C. Strom, *Transplantation* **82**, 441 (2006).
- 7) P. M. Miranda, V. Mohan, S. Ganthimathy, R. M. Anjana, S. Gunasekaran, V. Thiagarajan, T. A. Churchill, T. Kin, A. M. Shapiro, and J. R. Lakey, *Islets* **5**, 188 (2013).
- 8) F. Demachi, Y. Murayama, N. Hosaka, T. Mochizuki, K. Masuda, S. Enosawa, T. Chiba, Y. Oda, R. Suzuki, and K. Maruyama, *Jpn. J. Appl. Phys.* **54**, 07HF19 (2015).
- 9) T. Sawaguchi, F. Demachi, Y. Murayama, R. Oitate, S. Minakuchi, T. Mochizuki, and K. Masuda, Proc. 8th Biomedical Engineering Int. Conf., p. 1, 2015.
- 10) R. Oitate, A. Shimomura, H. Wada, T. Mochizuki, K. Masuda, Y. Oda, R. Suzuki, and K. Maruyama, *Jpn. J. Appl. Phys.* **56**, 07JF25 (2017).
- 11) R. Oitate, T. Otsuka, M. Seki, A. Furutani, T. Mochizuki, K. Masuda, R. Suzuki, and K. Maruyama, *Jpn. J. Appl. Phys.* **57**, 07JF10 (2018).
- 12) K. Masuda, T. Otsuka, M. Seki, R. Oitate, J. Unga, R. Suzuki, and K. Maruyama, Proc. IEEE Ultrasonics Symp., 2018, p. 1, [10.1109/ULTSYM.2018.8579669](https://doi.org/10.1109/ULTSYM.2018.8579669).
- 13) M. Seki, T. Otsuka, R. Oitate, K. Masuda, J. Unga, R. Suzuki, and K. Maruyama, *Jpn. J. Appl. Phys.* **58**, SGG13 (2019).
- 14) T. Saito, M. Seki, K. Nozaki, K. Masuda, Y. Miyamoto, D. Omata, and R. Suzuki, Proc. IEEE Ultrasonics Symp., 2020, p. 1, [10.1109/IUS46767.2020.9251363](https://doi.org/10.1109/IUS46767.2020.9251363).
- 15) K. Masuda, R. Nakamoto, N. Watarai, R. Koda, Y. Taguchi, T. Kozuka, Y. Miyamoto, T. Kakimoto, S. Enosawa, and T. Chiba, *Jpn. J. Appl. Phys.* **50**, 07HF11 (2011).
- 16) N. Shigehara, F. Demachi, R. Koda, T. Mochizuki, K. Masuda, S. Ikeda, F. Arai, Y. Miyamoto, and T. Chiba, *Jpn. J. Appl. Phys.* **52**, 07HF15 (2013).
- 17) N. Hosaka, R. Koda, S. Onogi, T. Mochizuki, and K. Masuda, *Jpn. J. Appl. Phys.* **52**, 07HF14 (2013).
- 18) R. Koda, J. Koido, T. Ito, T. Mochizuki, K. Masuda, S. Ikeda, F. Arai, Y. Miyamoto, and T. Chiba, *Jpn. J. Appl. Phys.* **52**, 07HF13 (2013).
- 19) K. Masuda, N. Hosaka, R. Koda, S. Miyazawa, and T. Mochizuki, Proc. IEEE Ultrasonics Symp., 2014, p. 1057, [10.1109/ULTSYM.2014.0259](https://doi.org/10.1109/ULTSYM.2014.0259).
- 20) T. Mochizuki, N. Tsurui, N. Hosaka, R. Koda, and K. Masuda, *Jpn. J. Appl. Phys.* **53**, 07KC09 (2014).
- 21) H. Ushimizu, T. Suzuki, T. Mochizuki, and K. Masuda, *Jpn. J. Appl. Phys.* **57**, 07LF21 (2018).
- 22) T. Hanmoto et al., *Biomed. Res.* **38**, 71 (2017).
- 23) T. Nishida, S. Kubota, E. Aoyama, N. Yamanaka, K. M. Lyons, and K. M. Takigawa, *Osteoarthritis Cartilage* **25**, 759 (2017).
- 24) H. Koibuchi, Y. Fujii, Y. Hirai, T. Mochizuki, K. Masuda, K. Kotani, T. Yamada, and N. Taniguchi, *J. Med. Ultrasonics.* **45**, 25 (2018).
- 25) A. Schuster, T. Schwab, M. Bischof, M. Klotz, R. Lemor, C. Degelb, and K. Schäfer, *Ann. Anatomy* **195**, 57 (2013).
- 26) F. Xu, X. Wang, N. Wu, S. He, W. Yi, S. Xiang, P. Zhang, X. Xie, and C. Ying, *Environ. Pollut.* **231**, 1609 (2017).
- 27) R. Suzuki, T. Takizawa, Y. Kuwata, M. Mutoh, N. Ishiguro, N. Utoguchi, A. Shinohara, M. Eriguchi, H. Yanagie, and K. Maruyama, *Int. J. Pharm.* **346**, 143 (2008).
- 28) Y. Negishi et al., *Biomaterials* **34**, 501 (2013).
- 29) X. Liu, L. Ruan, W. Mao, J. Q. Wang, Y. Shen, and M. Sui, *Int. J. Med. Sci.* **7**, 197 (2010).
- 30) Z. Chen, J. Deng, Y. Zhao, and T. Tao, *Int. J. Nanomed.* **7**, 3803 (2012).
- 31) X. Wu, F. Tian, M. Su, M. Wu, Y. Huang, L. Hu, L. Jin, and X. Zhu, *Int. Immunopharmacol.* **64**, 24 (2018).
- 32) Y. Ito, T. Saito, N. Kajita, Y. Miyamoto, R. Suzuki, K. Maruyama, D. Omata, and K. Masuda, Proc. The 42th Symp. on UltraSronics Electronics (2021), 3J1-3.
- 33) T. Katai, I. Yasuda, K. Watanabe, K. Okadome, Y. Edamoto, S. Enosawa, and K. Masuda, *IEEE Eng. Med. Biol. Soc.* 5824 (2019).